Postembryonic Localization of Allatotropin- and Allatostatin-Producing Cells in Central Nervous System of the Silk Moth Bmobyx mori

Authors: Park, Cheolin, Jeon, Sun Kyung, Kim, Min-Yung, Han, Sung Sik, Yu, Chai Hyeock, et al.

Source: Zoological Science, 18(3) : 367-379

Published By: Zoological Society of Japan

URL: https://doi.org/10.2108/zsj.18.367

ZOOLOGICAL SCIENCE **18**: 367–379 (2001)

Postembryonic Localization of Allatotropin- and Allatostatin-Producing Cells in Central Nervous System of the Silk Moth *Bmobyx mori*

Cheolin Park[1], Sun Kyung Jeon[1], Min-Yung Kim[2], Sung Sik Han[3], Chai Hyeock Yu[4] and Bong Hee Lee[1,3]*

[1]*Department of Biology, Korea University, Seoul 136-701, Korea,*
[2]*Research Institute of Basic Science, Korea University, Seoul 136-701, Korea*
[3]*Division of Biological Sciences, Graduate School of Biotechnology, Korea University, Seoul 136-701, Korea*
[4]*Department of Biology, Inha University, Inchon 402-751, Korea*

ABSTRACT—Polyclonal antisera to *Manduca sexta* allatotropin and allatostatin were utilized to localize allatotropin- and allatostatin-immunoreactivities in the central nervous system of larvae, pupae and adults from the silk moth *Bombyx mori*. In larva the first allatotropin-immunoreactivity appeared in the brain and terminal abdominal ganglion of first instar larva. In the third, fourth and fifth instar larvae, there was allatotropin-immunoreactivity in the suboesophageal ganglion, three thoracic ganglia, and eight abdominal ganglia with immunoreactivity in some axons of N 1 and N 2. Allatostatin-immunoreactivity, which could be not demonstrated in the first and second instar larvae, appeared first in the brain and suboesophageal ganglion of the third instar larva. Allatostatin-immunoreactive cells increased to seven pairs in brain of the fifth instar larva, in which immunreactivity also appeared in eight abdominal ganglia. Allatotropin- and allatostatin-immunoreactive cell bodies in the brain projected their axons into corpora allata without terminations in the corpora cardiaca. During pupal and adult stages, brains had no allatotropin-immunoreactivity in the brains, but most ventral ganglia contained allatotropin-immunoreactive cells. There was allatostatin-immunoreactivity in the brains of the 5- and 7-day-old pupae and adult and suboesophageal ganglion of the 7-day-old pupa.

INTRODUCTION

Metamorphosis, adult sexual maturation and reproduction of insects are controlled by precise hemolymph titers of juvenile hormone (JH) released from the corpora allata (CA) (Tobe and Stay, 1985). The biosynthesis of JH by the CA can be in turn controlled by the stimulatory neuropeptide allatotropin (AT) and inhibitory neuropeptide allatostatin (AST or allatoinhibin). These neurohormones are synthesized by neurosecretory cells in the brain and transported via nerves to the CA (Stay *et al*., 1992, 1994; Bellés *et al*., 1999). Therefore, AT and AST are involved in regulation of developmental changes by controlling JH biosynthesis and release in different insect species.

In addition, to stimulatory and inhibitory roles on JH biosynthesis and release, AT and AST were also demonstrated to exert other effects in the insects. The *Manduca sexta* allatotropin (Mas-AT) has a cardioacceleratory action on the pharate adult heart from *M. sexta* when it is released from specific neuronal cells in the abdominal ganglia (AG) (Veenstra *et al*., 1994). The callatostatins, which have been identified from head extracts of the blowfly *Calliphora vomitoria*, do not inhibit the dipteran form of JH biosynthesis and release by the CA (Duve *et al*., 1993). However, they have myoinhibitory effects on the blowfly hindgut (Duve and Thorpe, 1994; Duve *et al*., 1994) and the codling moth foregut (Duve *et al*., 1997a). The AST also seems to have roles in cockroach blood cells (Skinner *et al*., 1997) and in vitellogenin production (Martin *et al*., 1996).

To date, only one AT was isolated and characterized from *M. sexta* and this Mas-AT was described to be α-amidated tridecapeptide (Kataoka *et al*., 1989). However, a variety of ASTs have been identified from different insect species such as lepidopteran insects (Kramer *et al*., 1991; Duve *et al*., 1997b; Davey *et al*., 1999), blowfly (Duve *et al*., 1993), locust (Veelaert *et al*., 1996), and mosquito (Veenstra *et al*., 1997). In particular, fourteen isoforms of ASTs have been identified from cockroaches (Pratt *et al*., 1989, 1991; Woodhead *et al*., 1989, 1994; Donly *et al*., 1993; Bellés *et al*., 1994, 1999; Hayes

* Corresponding author: Tel. +82-2-3290-3156;
FAX. +82-2-923-9522.
E-mail: bhlee@mail.korea.ac.kr

et al., 1994; Stay *et al*., 1994; Weaver *et al*., 1994; Ding *et al*., 1995).

Most ASTs, including lepidostatin-1 (Davis *et al*., 1997) of *M. sexta*, range in size from 8 to 18 amino acids in various insect species and share the common C-terminal sequence of -Tyr-Xaa-Phe-Gly-Leu-NH_2. So far, two types of ASTs have been identified from *M. sexta*: one is the *M. sexta* allatostatin (Mas-AST) with full sequence of pGlu-Val-Arg-Phe-Arg-Gln-Cys-Tyr-Phe-Asn-Pro-Ile-Ser-Cys-Phe-OH (Kramer *et al*., 1991) and the other is the lepidostatin-1 with a C-terminal sequence YXFGLamide common in the cockroach ASTs (Davis *et al*., 1997).

AT is produced in cells of the larval brain of *M. sexta* (Žitňan *et al*., 1995; Taylor *et al*., 1996; Bhatt and Horodyski, 1999) and the larval and adult brains of *Drosophila melanogaster* (Žitňan *et al*., 1993). It is also synthesized from two pairs of median neurosecretory cells in the larval brain of the moth *Galleria mellonella* (Bogus and Scheller, 1994, 1996). AT-immunorective cells were also demonstrated in the suboesophageal ganglion (SOG), AG, terminal abdominal ganglion (TAG), frontal ganglion (FG), hypocerebral ganglion, proventricular ganglion, and midgut endocrine cells of *M. sexta* (Žitňan *et al*., 1993; Veenstra *et al*., 1994; Matthias and Klaus, 1995; Taylor *et al*., 1996; Bhatt and Horodyski, 1999). There was recently also a report on AT-immunoreactivity in terminals of locust thoracic sensory afferents (Persson and Nässel, 1999).

AST-producing cells show localizations in diverse insect tissues such as brain, SOG, thoracic ganglia (TG), AG, TAG, FG, midgut, and Malpighian tubules (Stay *et al*., 1992; Žitňan *et al*., 1993; Duve and Thorpe, 1994; Duve *et al*., 1994; Neuhäuser *et al*., 1994; Veelaert *et al*., 1995; Yoon and Stay, 1995; Žitňan *et al*., 1995; Vitzthum *et al*., 1996; Davis *et al*., 1997; Duve *et al*., 1997a; Audsley *et al*., 1998; Rankin *et al*., 1998; Maestro *et al*., 1998; Kreissl *et al*., 1999). ASTs are synthesized not only by neurosecretory cells (Neuhäuser *et al*., 1994) and interneurons (Duve and Thorpe, 1994) in the brain and/or SOG, but also by motoneurons in the TG or TAG (Yoon and Stay, 1995; Davis *et al*., 1997; Kreissl *et al*., 1999).

The AT-immunoreactive cells in *D. melanogaster* changes in localization and number during postembryonic development (Žitňan *et al*., 1993). Studies using antisera against Mas-AT and Mas-AST revealed that the number and localization of immunoreactive neurons in the developing CNSs of *M. sexta* differs from that in *D. melanogaster* (Žitňan *et al*., 1993, 1995; Bhatt and Horodyski, 1999). In *M. sexta* Mas-AT-immunoreactive (Mas-AT-IR) cells could be detected from brain, SOG and TAG of larva, and AG and TAG of pupa and pharate adult. In 5th instar larva from *M. sexta,* the number of Mas-AT-IR neurons increases and the number of Mas-AST-immunoreactice (Mas-AST-IR) neurons decreases (Žitňan *et al*., 1995).

To compare localization of AT- and AST-producing neurons in the CNS of an insect, Mas-AT- and Mas-AST-immunoreactivities are described in the neurons of developing CNS in the silk moth *B. mori*.

MATERIALS AND METHODS

Insects

Cold-treated eggs from the silk moth *Bombyx mori*, which were kindly provided from National Institute of Agriculture, Science and Technology, Suwon), were hatched to 1st instar larvae about 10 days after incubation at 28°C and relative humidity of 70%. The 1st instar larvae, reared on an artificial diet (made mainly by mulberry leaves and essential minerals) purchased commercially, were ecdysed to 2nd, 3rd, 4th, and then 5th (last) instar larvae under the conditions described above. The larval life of the silk moth lasts for about three weeks prior to metamorphosis of larvae to the pupae. After about-10-days pupal life, pupae emerged to adults. Insects used were 1st, 2nd, 3rd, 4th, 5th instar larvae, 3-, 5- and 7-day-old pupae as well as 1-day-old adults, collected from a stock colony kept in the laboratory. In case of the 5th instar larva, day-1 larvae were selected. Both elapsed day after the egg hatching (under the rearing conditions mentioned above) and head size were two crucial criteria to discriminate the staging of the 1st, 2nd, 3rd, 4th and 5th instar larvae.

Antibodies

We used antisera raised against *M. sexta* allatotropin and allatostatin (Mas-AT and Mas-AST) neuropeptides. Rabbit anti-Mas-AT was kindly provided by Dr. J. A. Veenstra (Universite Bordeaux 1, France) and has been previously characterized by Veenstra and Hagedorn (1993). Rabbit anti-Mas-AST was made by Josman Laboratories (Napa, CA) in collaboration with Dr. S. J. Kramer and then kindly given to us by Sandoz Crop Protection (Palo Alto, CA). Characterization of the anti-Mas-AST antibodies has been described previously by Žitňan *et al.* (1995).

Wholemount immunocytochemistry

Tissue preparation and immunocytochemistry were carried out as described from Kim *et al.* (1998). The CNS including retrocerebral complex (CC–CA) from each developing stage described above was rapidly dissected and then isolated in 0.1M sodium phosphate buffer (pH 7.4) and fixed in 4% paraformaldehyde (PFA) in 0.1M sodium phosphate buffer for 5–9 hr at 4°C, depending on size of each tissue. After thorough washes in 0.1M phosphate-buffered saline (PBS) with 1% Triton X-100 (Tx) at room temperature overnight the tissues were incubated in either of the two primary antibodies (anti-Mas-AT and anti-Mas-AST) diluted to 1:1,500 in dilution buffer with 0.01M PBS with 0.25% Tx and 10% normal serum for 4–5 days. The tissues were followed by thorough washes in 0.1M PBS with 0.25% Tx. The binding of anti-Mas-AT or anti-Mas-AST to the tissue was detected by the peroxidase-antiperoxidase (PAP) method for wholemount as described by Lee *et al.* (1998). As a specificity control immunocytochemistry was performed on whole tissues of brain-CC-CA and all ganglia of ventral nerve cord with anti-Mas-AT and anti-Mas-AST preincubated for 24 hr with 50 nmol synthetic Mas-AT and Mas-AST/ml diluted antiserum (diluted to 1:1,500).

Fluorescence immunocytochemistry

Ventral ganglia including the eight AG were isolated in 0.1M sodium phosphate buffer, fixed in 4% PFA for 4 hr at 4°C, and washed with 80% ethanol (8×10 min). Further wash was followed in 0.1M PBS with 0.25% Tx (4×10 min), and tissues were then incubated with anti-Mas-AT (diluted to 1:1,000 in 0.01M PBST with 10% normal serum) overnight at room temperature. They were rinsed in 0.01M PBST (5×10 min) and then incubation with swine anti-rabbit IgG conjugated with FITC followed for 4 hr at room temperature in darkness at 4°C. Tissues were finally washed in 0.1M PBS with 0.25% Tx (3×10 min), embedded in glycerin, examined and photographed with a Nikon fluorescence microscope.

RESULTS

There were no immunoreactive nervous or axonal process in the brain-CC-CA or in any of the ganglia of ventral nerve cord when applying the Mas-AT and Mas-AST antisera preabsorbed with 50 μM synthetic Mas-AT and Mas-AST. The immunoreactive cells of the larvae, pupae and adults will be described below, starting with the brain-CC-CA and subsequently continuing to ventral nerve cord.

Mas-AT- and Mas-AST-IR neurons in the brain-CC-CA

At least five immunoreactive specimens were investigated at each developmental stage. In general, immunoreactivity with the antiserum against Mas-AT was not strong especially in the brain, while immunoreactivity with antiserum against Mas-AST was intensive. General localization and number of both Mas-AT-IR and Mas-AST-IR cell bodies or neurons in the brains (including CC-CA) are shown in Fig. 1 and Table 1.

In the 1st and 2nd instar larval brains there were Mas-AT-IR cell bodies, but no Mas-AST-IR cell body. In the 1st instar larva, there were four pairs of Mas-AT-IR cell bodies in the medial and lateral parts of the brain (Fig. 1A, 2A). In addition to these cell bodies, two pairs of cells, which were regarded as median neurosecretory cell, were localized also in the pars intercerebralis of the protocerebrum in the 2nd instar larval brain (Fig. 1B). In the 3rd to 5th instar larvae, both Mas-AT-IR and Mas-AST-IR cell bodies could be found together throughout the brain (Fig. 1C, D, E). From the 3rd instar larva, the two pairs of Mas-AT-IR median neurosecretory cells found in the medial part from the 2nd instar larval brain were no longer immunoreactive. One pair of Mas-AT-IR cell bodies newly appeared in the ventrolateral part of 3rd instar larval brain (Fig. 1C, 2B). Compared with the scattered distribution of five pairs of Mas-AT-IR cell bodies in the 3rd instar larval brain (Fig. 1C, 2B), three pairs of Mas-AST-IR cell bodies showed a clustered localization in the pars lateralis of the protocerebrum as shown in Fig. 3B. There was no change in number of Mas-AT-IR cell bodies in the 4th instar larval brain, whereas they showed changes in localization. Five pairs of Mas-AT-IR cell bodies could be seen in this larval stage. At this stage three pairs near the medial part of the brain, seen in earlier stages, were no longer immunoreactive and one pair in the pars intercerebralis appeared (Fig. 1D). However, Mas-AST-IR cell bodies showed no changes in the number and localization in the 4th instar larval brain. As seen in Fig. 1E, 5th instar larval brain contained an increased number of immunoreactive cell bodies. About ten pairs of Mas-AT-IR cell bodies were dispersed in the pars intercerebralis, near the medial part and in the ventrolateral part of the brain (Fig. 2C), while seven pairs of Mas-AST-IR cell bodies continuously showed a clustered localization in the pars lateralis (Fig. 3C), as in the previous larval stages.

The CA contained Mas-AT-IR processes (including axon terminals) which were perhaps originated from labeled cerebral cell bodies (Fig. 2D). However, antiserum against Mas-AT failed to label these axonal pathways in the 5th instar larval brain. In contrast, long labeled axons were revealed by reaction with antiserum against the Mas-AST in the brain and retrocerebral complex of the 5th instar larva (Fig. 3D, E, F). Those axons that originated from Mas-AST-IR cell bodies in the pars lateralis of the protocerebrum were extended to the CA in which they eventually terminated. For innervation to ipsilateral CA, they passed through NCC II, CC and NCA I (Fig. 3E, arrowheads). Mas-AST-IR axons showed extensive arborization within the CA (Fig. 3F). In the CC, however, there were no axon terminals labeled by either antiserum.

During the pupal and adult stages, Mas-AT-IR cells could not be detected in the brain. However, Mas-AST-IR cells were found in one pair of cell bodies in the pars lateralis of the protocerebrum from the 5-, 7-day-old pupal and 1-day-old adult brains, respectively (Fig. 1F, G, 4A). As shown in Fig. 4b, there were two pairs of Mas-AST-IR cell bodies in the 7-day-old-pupal SOG fused earlier to the brain. But these cell bodies disappeared from the brain-SOG complex of 1-day-old adult.

Mas-AT-IR and Mas-AST-IR neurons in the ventral nerve cord

At least five immunoreactive specimens were investigated at each stage for detection of labeled neurons in the ganglia of the ventral nerve cord. During the larval life, there were Mas-AT-IR cells in most ganglia of the ventral nerve cord, but Mas-AST-IR cells could be demonstrated only in restricted ganglia of ventral nerve cord of 3rd, 4th and 5th instar larvae (Fig. 5, Table 1). During the pupal and adult stages, Mas-AT-IR cells were successively seen in most of the ventral ganglia. However, there were Mas-AST-IR cells only in the SOG of 7-day-old pupa.

In the 1st instar larva, there were about 8 Mas-AT-IR cell bodies only in TAG. Four large immunoreactive cell bodies were localized in the center of AG 7 neuromere and another four were distributed in the posterior part of 8th neuromere of the TAG. One pair and four pairs could be also seen in the anteromedian portion of the SOG and TAG of the 2nd instar larva, respectively. In the 3rd instar larva there was an increase in the number of Mas-AT-IR cell bodies in the ganglia of the ventral nerve cord. All ventral ganglia had Mas-AT-IR cell bodies. There were four pairs of immunoreactive cell bodies in the anteromedian, middle and posteromedian portions of the SOG, two pairs in the middle and posterior portions of the TG 1, two pairs in the middle and posterior portions of the TG 2, and three pairs in the anteromedain and posterormedian portion of the TG 3. In the AG, one pair of Mas-AT-IR cell bodies was seen in the posteromedian portions of each of AG 1, 2, 3, 4, 5 (Fig. 5) and 6, and two pairs and 4 midline cells also in the TAG. In this stage, only SOG of the ventral ganglia had one pair of Mas-AST-IR cell bodies. There were the same number and localization of Mas-AT-IR cell bodies in all ventral ganglia from the 4th and 5th instar larvae as from the 3rd instar larva (Fig. 5, 6A, B, C, D, 7A, B). As in Fig. 8, each of AG 1 to 7 contained Mas-AT-IR cells in the anterior neuropil and two Mas-AT-IR cell bodies in the posteromedian portion.

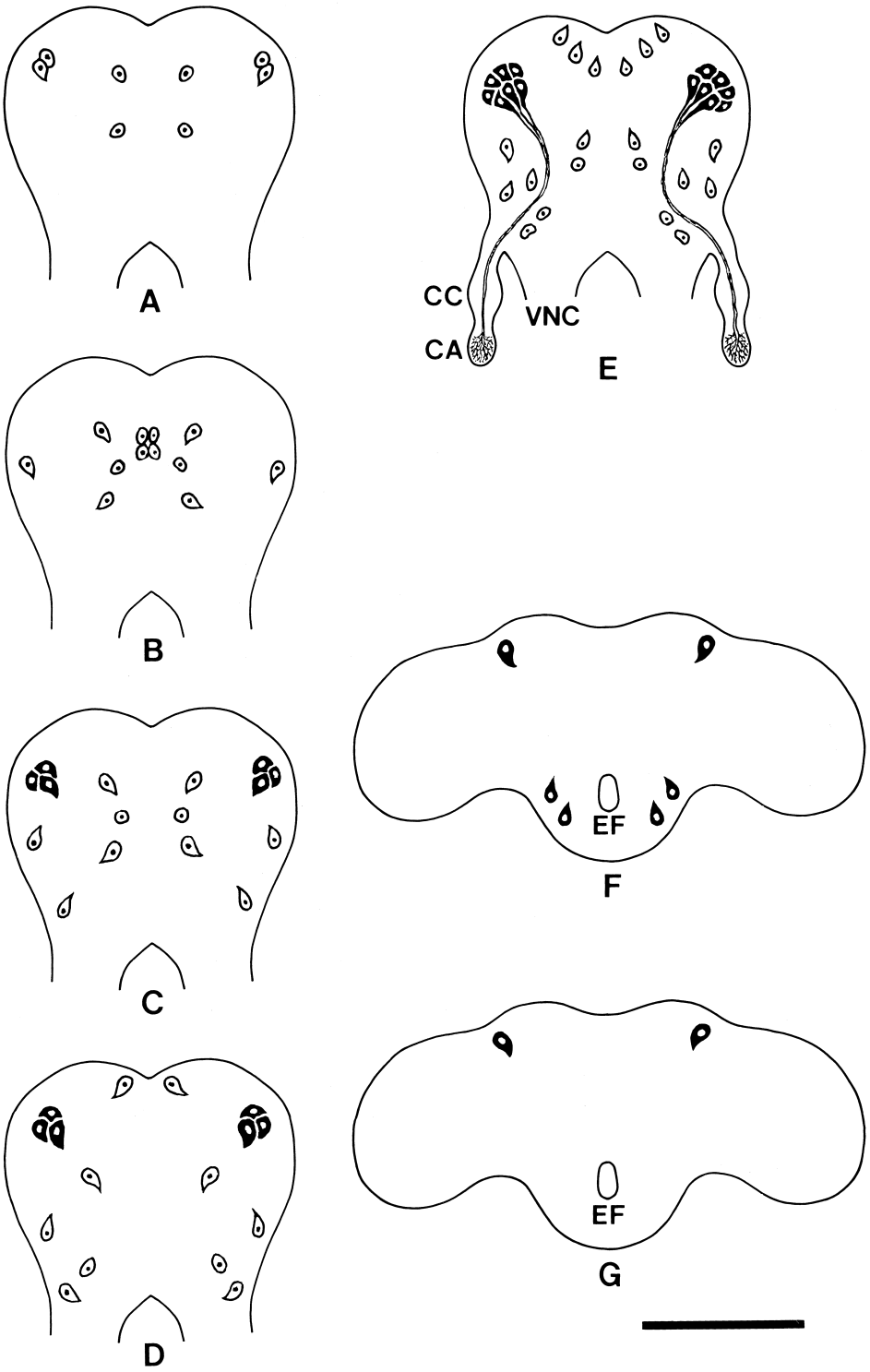

Fig. 1. Schematic tracings of Mas-AT-IR and Mas-AST-IR cell bodies in the larval, pupal and adult brains from *Bombyx mori*, including projection of Mas-AST-IR neurons into the fifth instar larval CA, drawn from whole-mount; only clearly labeled cells have been drawn. Pear-like structure with unfilled surrounding, Mas-AT-IR cell body; pear-like structure with filled surrounding, Mas-AST-IR cell body. Scale bar indicates 0.5mm. A. 1st instar larval brain including four pairs of Mas-AT-IR cell bodies. B. 2nd instar larval brain showing six pairs of Mas-AT-IR cell bodies. C. 3rd instar larval brain including five pairs of Mas-AT-IR cell bodies. Three Mas-AST-IR cell bodies are grouped into a lateral portion. D. 4th instar larval brain containing five pairs of Mas-AT-IR cell bodies and three pairs of Mas-AST-IR cell bodies. E. 5th instar larval brain including ten pairs of Mas-AT-IR cell bodies and seven pairs of Mas-AST-IR cell bodies. Note that Mas-AT-IR cell bodies are dispersed, but Mas-AST-IR neurons are aggregated to a portion in the pars lateralis of the protocerebrum. Mas-AST-IR neurons project their axons in the CA, in which axons of the neurons abundantly arborize. F. 5-day-old pupal brain including one pair of Mas-AST-IR cell bodies and suboesophageal ganglion containing two pairs of Mas-AST-IR cell bodies. EF, esophageal foramen. G. 1-day-old adult showing one pair of Mas-AST-IR cell bodies.

Table 1. Comparison of number of Mas-AT-IR cells and Mas-AST-IR cells in developing CNS of *Bombyx mori*

	1st IL	2nd IL	3rd IL	4th IL	5th IL	P-3	P-5	P-7	Adult
Br	8/–	12/–	10/6	10/6	20/14	–/–	–/2	–/2	–/2
SOG	–/–	2/–	8/2	8/2	8/4	8/–	–/–	–/4	–/–
TG1	–/–	–/–	4/–	4/–	4/–	4/–	2/–	2/–	2/–
TG2	–/–	–/–	4/–	4/–	4/–	4/–	4/–[1]	4/–[1]	4/–[1]
TG3	–/–	–/–	6/–	6/–	6/–	6/–			
AG1	–/–	–/–	2/–	2/–	2/2	2/–			
AG2	–/–	–/–	2/–	2/–	2/2	2/–			
AG3	–/–	–/–	2/–	2/–	2/2	2/–	2/–	2/–	2/–
AG4	–/–	–/–	2/–	2/–	2/2	2/–	2/–	2/–	2/–
AG5	–/–	–/–	2/–	2/–	2/2	2/–	2/–	2/–	2/–
AG6	–/–	–/–	2/–	2/–	2/2	2/–	8/–[2]	8/–[2]	8/–[2]
TAG	8/–	8/–	8/–	8/–	8/4[3]	8/–			

Note : Mas-AT-IR cells/Mas-AST-IR cells

Keys : Br, brain; SOG, suboesophageal ganglion; TG 1-3, thoracic ganglion 1-3; AG 1–8, abdominal ganglion 1-8; 1st to 5th IL, 1st instar larva to 5th instar larva; P-3, P-5 and P-7, 3-, 5- and 7-day-old pupae; [1]AG 1 and AG 2 are fused with TG 2 and 3, forming pterygothoracic ganglion; [2]AG 6 is fused with AG 7/8, forming TAG; [3]Numbers of Mas-AT-IR cells and Mas-AST-IR cells found commonly in more than four of at least five individuals investigated in each developmental stage.

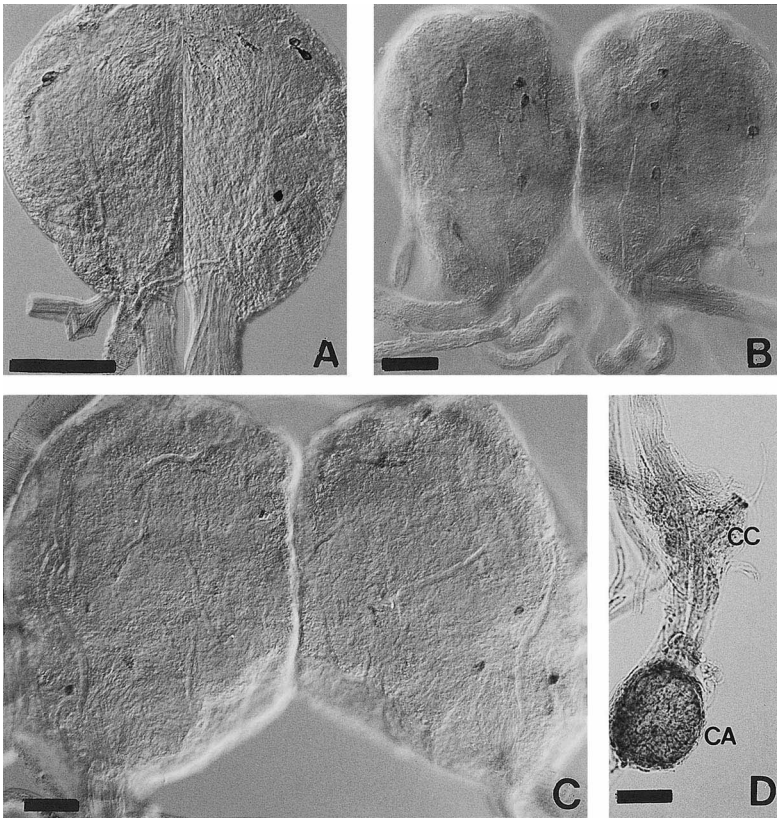

Fig. 2. Mas-AT-IR in the different larval brains and fifth instar larval retrocerebral complex. A. Mas-AT-IR cell bodies in lateral portion of 1st instar larval brain. Scale bar indicates 50 μm. B. 3rd instar larval brain with five pairs of Mas-AT-IR cell bodies. Scale bar indicates 50 μm. C. 5th instar larval brain with Mas-AT-IR cell bodies. Scale bar indicates 50 μm. D. Retrocerebral complex of 5th instar larva. Note that CA shows Mas-AT-IR in the peripheral portion but CC display no Mas-AT-IR. Scale bar indicates 50 μm

The Mas-AT-IR cells in AG 1 to 7 showed similarity in their appearance. Mas-AT-IR axons in the nerve 1 and 2 (N 1 and N 2) originating from AG 1 to 7 were derived mostly from two ganglionic labeled cell bodies and ran through the portion of Mas-AT-IR in each neuropil of those ganglia (Fig. 8A, B, C, D) (see Burrows (1996) for definition of the nerves N 1 and 2). In the 5th instar larva, there were two pairs of bilateral Mas-AST-IR cell bodies in the middle of the SOG (Fig. 5A). There was also one bilateral pair in the middle portion of each of AG 1 to 6, respectively (Fig. 5E–J, 9A, B). One bilateral pair of Mas-AST-IR axons ran longitudinally in the central neuropils of the AG, as seen in Fig. 9. Two bilateral pairs of Mas-AST-IR cell

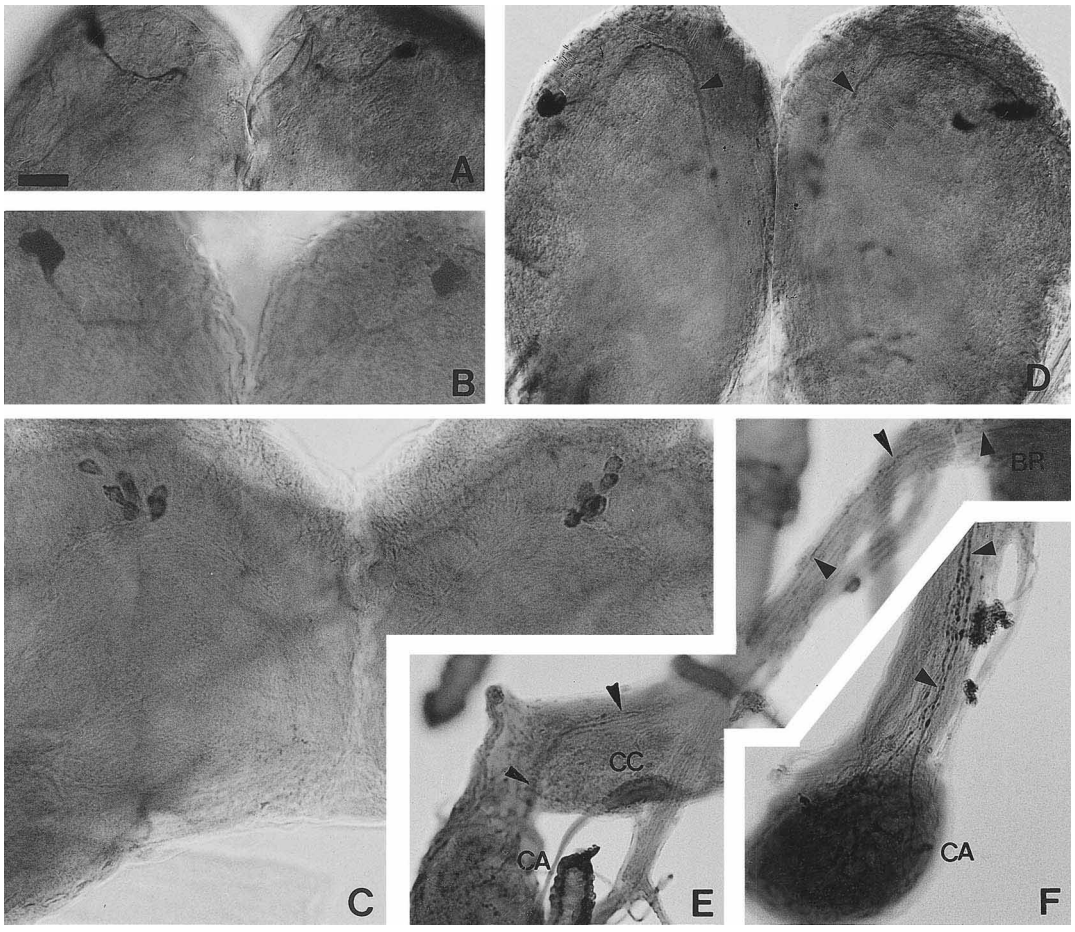

Fig. 3. Mas-AST-IR in the different larval brain and projection of Mas-AST-IR neurons from brain into CA in 5th instar larva. Magnification of all photographs is same as in Fig. 4A. A. 3rd instar larval brain. There are three pairs of Mas-AST-IR cells. Scale bar indicates 50 μm. B. 4th instar larval brain. Note that the brain has the same number of Mas-AST-IR cells as in the 3rd instar larval brain. C. 5th instar larval brain including seven pairs of bilateral Mas-AST-IR cell bodies in the lateral portion of the protocerebrum. D. 5th instar larval brain showing Mas-AST-IR neurons projecting their axons (arrowheads) from cell bodies in the lateral portions toward retrocerebral CA in two cerebral hemispheres, respectively. E. Mas-AST-IR cerebral neurons showing innervation of axons to CA through NCC I+II, CC, and NCA I in the 5th instar larva. A few Mas-AST-IR axons (arrowheads) are projected from the brain (Br) into the CA without termination in the CC. F. Magnified CA and NCA I showing projection of a few Mas-AST-IR axons (arrowheads) into the CA through NCA I. The CA contains strongly labeled, rich axon terminals.

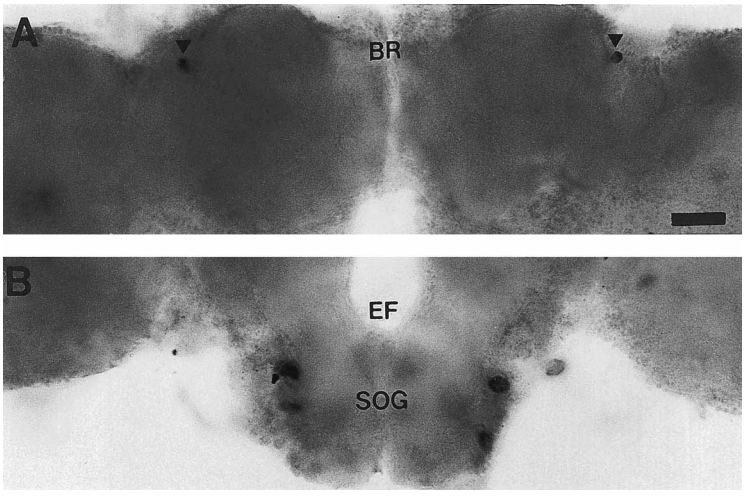

Fig. 4. Mas-AST-IR in the brain (Br) and SOG of 7-day-old pupa. A. Brain has one pair of bilateral Mas-AST-IR cell bodies (arrowheads) in the lateral portion of the protocerebrum. Scale bar indicates 50 μm. B. SOG contains two pairs of bilateral AST- immunoreactive cell bodies in the lateral portion. Magnification is same as in Fig 5A. EF, esophageal foramen.

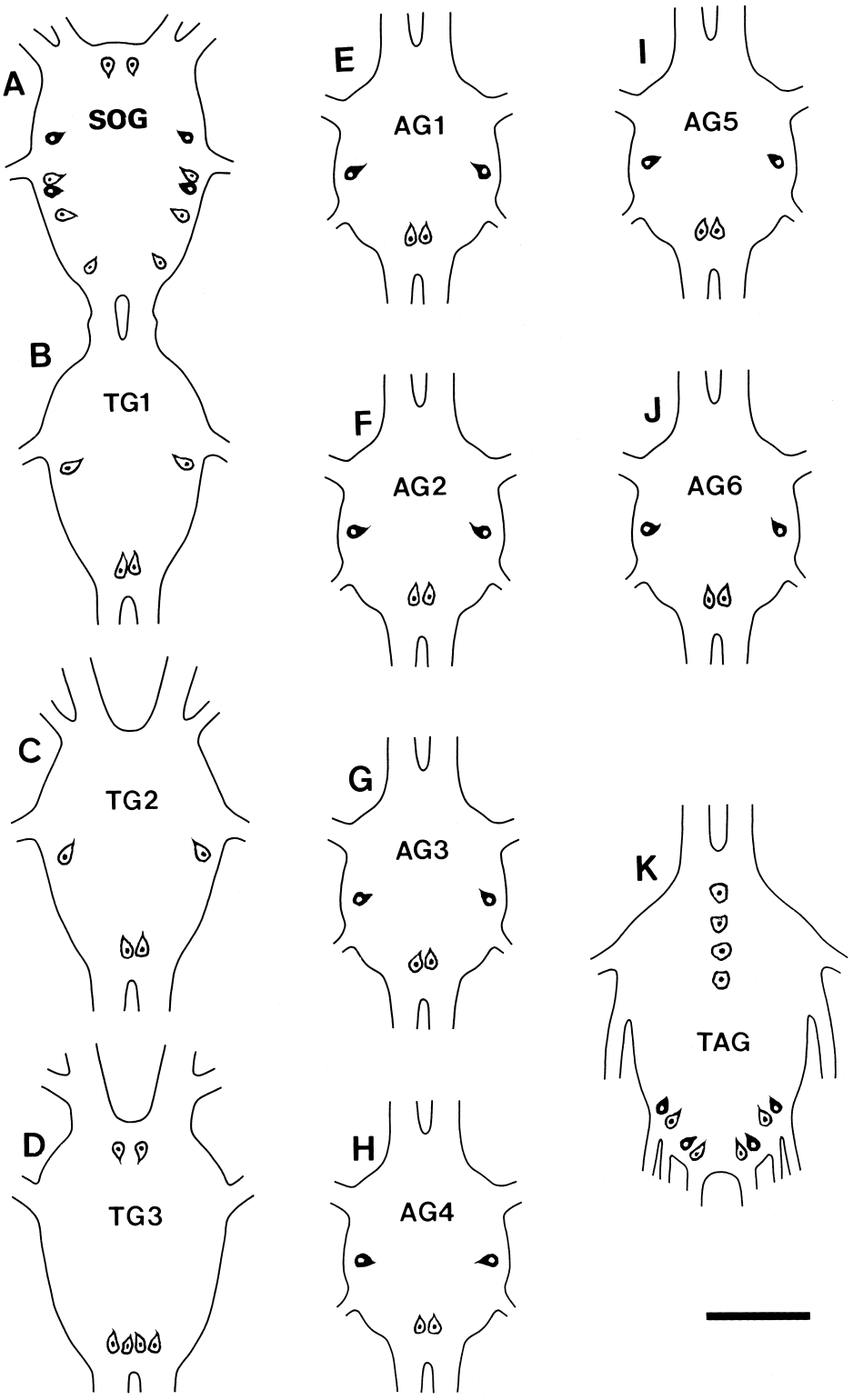

Fig. 5. Schematic tracings of Mas-AT-IR and Mas-AST-IR cell bodies in the ventral ganglia of the fifth instar larvae of *Bombyx mori*, drawn from whole-mount; only clearly labeled cell bodies have been drawn. Pear-like structure with unfilled surrounding, Mas-AT-IR cell body; pear-like structure with filled surrounding, Mas-AST-IR cell body. Scale bar indicates 1 mm. A. Suboesophageal ganglion (SOG) containing four pairs of Mas-AT-IR cell bodies and two pairs of Mas-AST-IR cell bodies. B. Prothoracic ganglion (TG 1). C. Mesothoracic ganglion (TG 2). Two pairs of Mas-AT-IR cell bodies are located in the same position of TG 1 and TG 2, respectively. D. Metathoracic ganglion (TG 3). E. First abdominal ganglion (AG 1). F. Second abdominal ganglion (AG 2). G. Third abdominal ganglion (AG 3). H. Fourth abdominal ganglion (AG 4). I. Fifth abdominal ganglion (AG 5). J. Sixth abdominal ganglion (AG 6). In AG 1 to 6, there is one pair of Mas-AT-IR cell bodies in each posteromedian portion, whereas one pair of Mas-AST-IR cell bodies is located in each middle portion. K. Terminal abdominal ganglion (TAG) showing four large Mas-AT-IR cell bodies in the 7th neuromere and two pairs of Mas-AT-IR cell bodies and two pairs Mas-AST-IR cell bodies in the 8th neuromere.

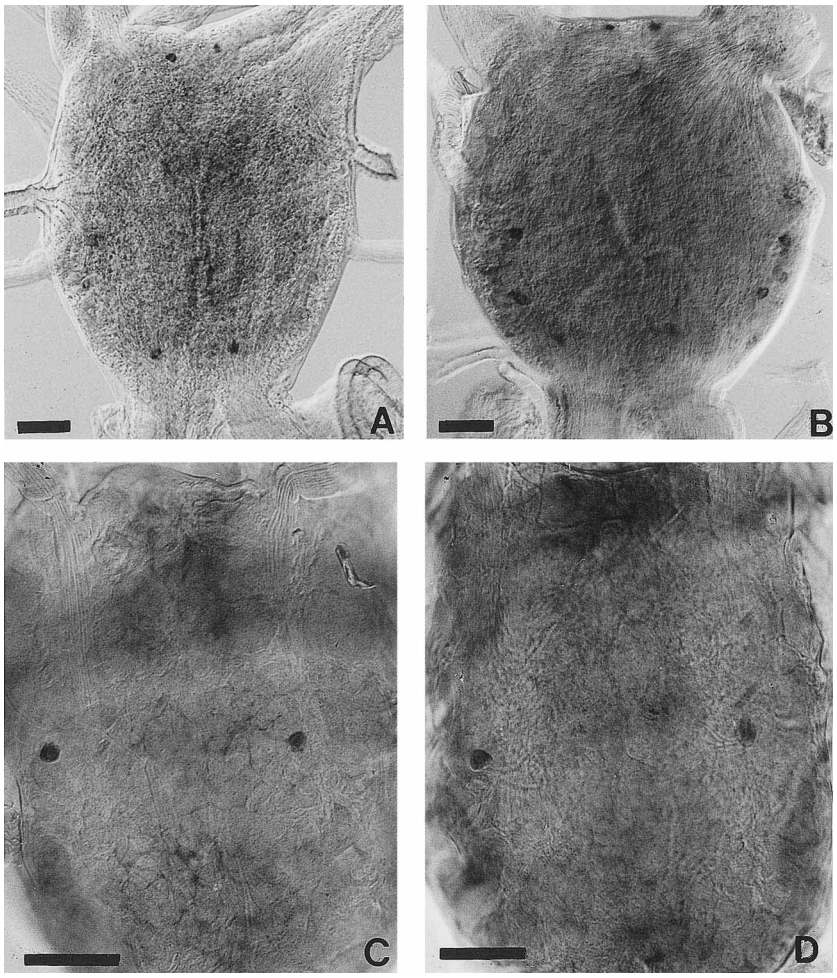

Fig. 6. Mas-AT- and Mas-AST-IR in the larval SOG. A. SOG of 4th instar larva showing Mas-AT-IR cell bodies in both anteromedian and posteromedian portions. Scale bar indicates 50 μm. B. SOG of 5th instar larva containing four pairs of bilateral AT-IR cell bodies in the different portions. Scale bar indicates 50 μm. C. SOG of 4th instar larva showing AST-IR cell bodies in the lateral portion. Scale bar indicates 50 μm. D. SOG of 5th instar larva containing one pair of AST-IR cell bodies as in the 4th instar larval SOG. Scale bar indicates 50 μm.

bodies could be also demonstrated in the posterior portion of AG 8 neuromere of the TAG (Fig. 5K).

In the pupal and adult stages, there were Mas-AT-IR cell bodies in most of the ventral ganglia. But Mas-AST-IR cell bodies could be not seen in most ventral ganglia (data not shown). Although the SOG had two pairs of Mas-AST-IR cell bodies in the 7-day-old pupa (Fig. 4B), it has already been fused with the brain from the 5-day-old pupa. Number, localization and axonal projection of Mas-AT-IR cell bodies in the ventral ganglia of the 3-day-old pupa were the same as those in the larval ventral ganglia, as shown in AG 3 of Fig. 8D. In the TG of the 5- and 7-day-old pupae and adult, Mas-AT-IR cells showed the changes in their number and localization due to the formation of the pterothoracic ganglion (PTG) by fusion of TG 2 and 3 with AG1 and 2 in the 5-day-old pupa. TG 1 had one pair of Mas-AT-IR cell bodies in the middle portion. In the PTG, there was also one pair of immunoreactive cell bodies in the lateral portion of TG 2 neuromere, one pair in the median portion of TG 3 neuromere, and one pair in the median portion of AG 2 neuromere, respectively. However, the pattern of number and localization of these cell bodies in the AG 1 to 5 and TAG was the same as that in the 3-day-old pupa.

DISCUSSION

Mas-AT-IR and Mas-AST-IR cells were distributed in distinct sets of neurons of the CNS of the moth *B. mori*, respectively. Mas-AT-IRs was seen in all ganglia during a wider range of postembryonic stages, whereas Mas-AST-IR could be demonstrated in some ganglia of the CNS in a more restricted range of postembryonic stages (see Fig. 1). Thus there were a relatively larger number of Mas-AT-IR cells throughout the CNS, compared to a very restricted number of Mas-AST-IR cells (see Table 1). It has been shown that several insect species investigated also showed distinct distributions of AT- and AST-IR cells throughout the CNS, with some similarities in the localization (Stay *et al.*, 1992; Žitňan *et al.*, 1993, 1995; Bhatt and Horodyski, 1999).

In the 5th instar larva of *B. mori,* ten pairs of Mas-AT-IR

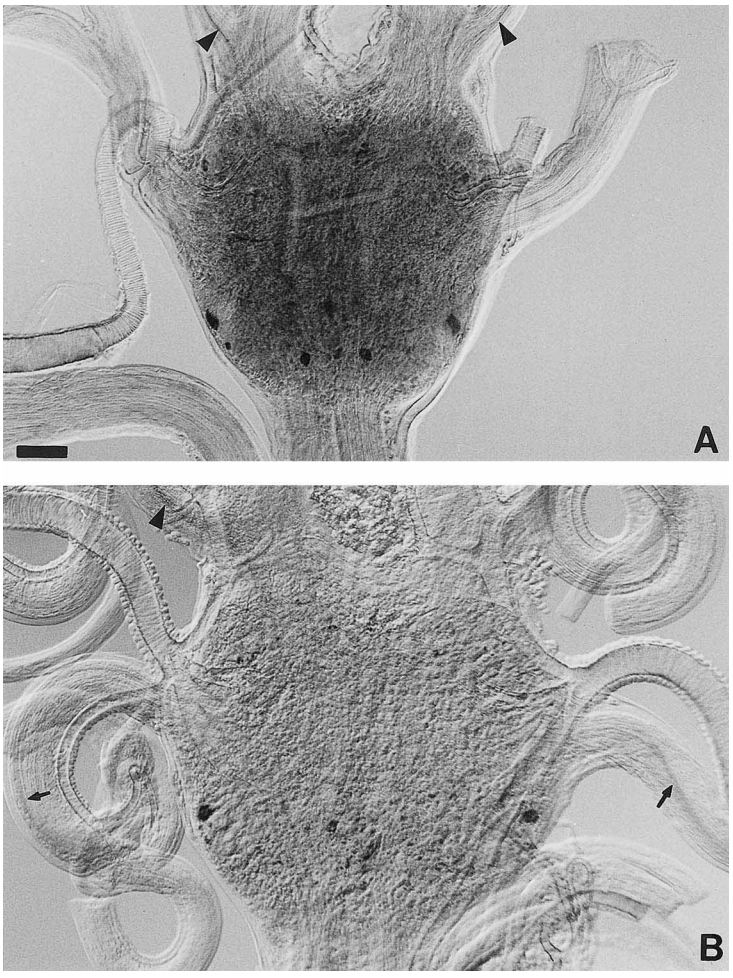

Fig. 7. Mas-AT-IR in the TG. A. TG 2 of 4th instar larva showing two pairs of AT-IR cell bodies in the posterior portion. Note that one pair of anterior nerves extended from the TG 2 contains labeled axons (arrowheads). Scale bar indicates 50 μm. B. TG 2 of 5th instar larva containing one pair of labeled cell bodies in the lateral portion. Axons in the anterior (arrowhead) and posterior (arrows) nerves from TG 2 are labeled with the AT. Magnification is same as in Fig. 7A.

cell bodies were dispersed in the brain, whereas seven pairs of Mas-AST-IR cells were localized in a group in the brain. The ten pairs of Mas-AT-IR neurons in the 5th instar larval brain were those that have gradually increased from four pairs in the 1st instar larval brain. In contrast, Mas-AST-IR cells abruptly increased in numbers from four pairs in the 4th instar larval brain to seven pairs in the 5th instar larval brain. There were no Mas-AST-IR cells in the 1st to 3rd instar larval brains and also no numerical change of these cells between the 3rd and 4th instar larval brains. It has been demonstrated that during the 5th instar larval stage of *M. sexta* these Mas-AT-IR cells show a drastic decrease in number in the transition period from earlier to later substages (Bhatt and Horodyski, 1999). From these data, it was assumed that relative changes in numbers of Mas-AT-IR cells and Mas-AST-IR cells in the brains during all the larval lives might directly influence the JH biosynthesis and release by the CA. It was suggested that in *B. mori* production of only Mas-AT without synthesis Mas-AST in the brains during early larval stages caused stimulation of JH biosynthesis in the CA. During the 5th instar larva, however, a gradual decrease of Mas-AT-IR cells but successive presence of Mas-AST in the brain perhaps leaded to a gradual inhition of JH biosynthesis.

In the 5th instar larval brain of *B. mori*, there was abundant Mas-AT- and Mas-AST-immunoreactivities in the CA. In particular, Mas-AST-labeling could be in axon terminals originating from immunoreactive cell bodies in the brain (not shown). Different insect species showed distinct differences in the morphology of AT- and AST-labeled neurons termination in the retrocerebral complex. In *B. mori*, the CA is the main accumulation and release sites of both Mas-AT and Mas-AST transported from the brain neurosecretory cells, as in adult *D. punctata* (Stay *et al*., 1992). However, *D. punctata*-AST-immunoreactivity could be shown in the CC of the 5th instar larva from *B. mori* and there was no *D. punctata*-AST-immunoreactivity in the CA (Jin *et al*., 2000). In the retrocerebral complex of *B. mori*, it was demonstrated that Mas-AST-labeling and *D. punctata*-AST-labeling showed distinct distribution patterns. This suggested the presence of two types of ASTs, each in a distinct neurosecretory system. In *G.*

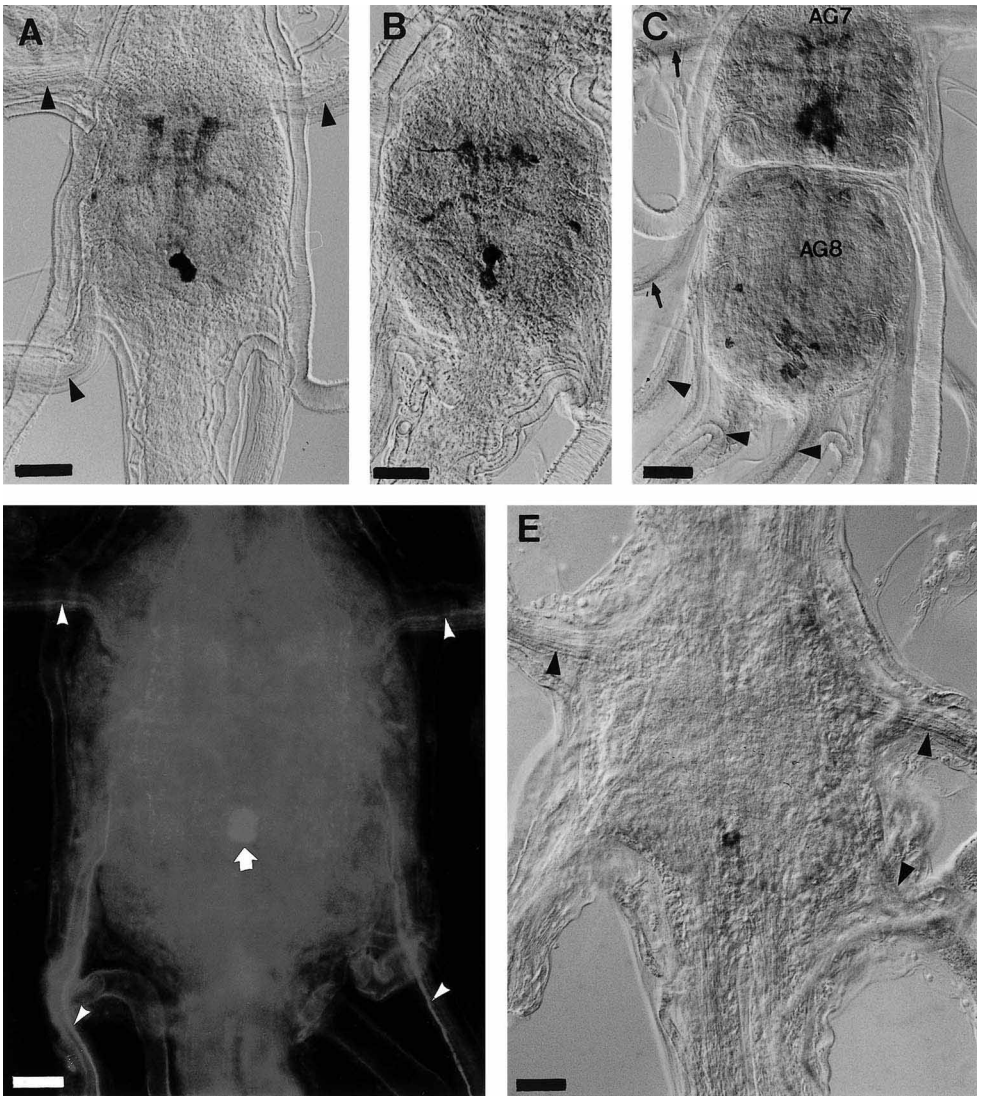

Fig. 8. Mas-AT-IR in the AG. A. AG 1 of 5th instar larva containing two labeled cell bodies in the posteromedian portion. It has two Mas-AT-IR cell bodies and Mas-AT-IR, which is similar in the appearance in the neuropils of AG 1 to 7. Note that Mas-AT-IR axons (arrowheads) could be detected within the N 1 and N 2. Scale bar indicates 50 μm. B. AG 2 of 5th instar larva. This Mas-AT-IR in those AG reveals abundant processes originated from two Mas-AT-IR cell bodies. Scale bar indicates 50um. Scale bar indicates 50 μm. C. TAG of 5th instar larva. There are four Mas-AT-IR cell bodies and Mas-AT-IR in the AG 7, which is similar to that in the AG 1 to 6. Note that N 1 and N 2 extended from the AG 7 have Mas-AT-IR axons (arrows) and most of the nerves extended from AG 8 contain also Mas-AT-IR axons (arrowheads). Scale bar indicates 50 μm. D. AG 3 of 5th instar larva containing two FITC-labeled, Mas-AT-IR cell bodies (arrow) in the posteromedian portion of the ganglion and labeled axons (arrowheads) in the N 1 and N 2. Localization of two Mas-AT-IR cell bodies in the AG 3 and projection of ganglionic Mas-AT-IR neurons to the N 1 and N 2 are same as those in the AG 1 to 2 and 4 to 6. Scale bar indicates 50 μm. E. AG 4 of 3-day-old pupa showing same localization of Mas-AT-IR cell body and same axonal projection of ganglionic Mas-AT-IR neurons into the N 1 and N 2 (arrows) as in the larval AG 4. Scale bar indicates 50 μm.

mellonella, the CC is a main site for accumulation and release of the AT from two pairs of median neurosecretory cells in the pars intercerebralis (Bogus and Scheller, 1994, 1996). This AT release from the CC was shown to stimulate JH biosynthesis by the CA. Thus *B. mori* showed a different pattern in accumulation and release sites of the AT compared to that in *G. mellonalla*, although they belonged to the same lepidopteran insects. In *M. sexta* there are Mas-AT-IR axons within both CC and CA, but Mas-AST-IR neurons, whose cell bodies are located in the brain, project their axons into the CA without termination in the CC. (Žitňan *et al*., 1995). In *Cydia pomonella* the AST-IR is normally accumulated in the CC, but not in the CA (Duve et al., 1997a), as in *G. mellonella*. In *Schistocerca gregaria* and *Locusta migratoria* and *Acheta domesticus*, both CC and CA accumulate and release the AST transported from the brain, but in fleshfly *Neobellieria bullata* the ASTs are accumulated in neither the CC or the CA (Neuhäuser *et al*., 1994; Veelaert *et al*., 1995). It has been also demonstrated that in adult *D. melanogaster* the nerves, which extend from the brain to the CA, are not AST-IR (Yoon and Stay, 1995).

The first Mas-AT-immunoreactivity in *B. mori* TG appeared

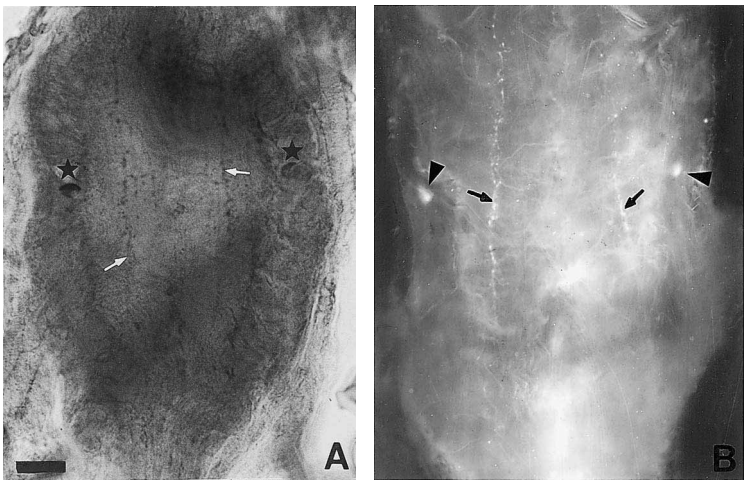

Fig. 9. Mas-AST-IR in the larval AG. A. AG 1 of the 5th instar larva. There is one pair of bilateral Mas-AST-IR cell bodies (stars) in the middle portion and one pair of Mas-AST-IR axons (white arrows) interconnecting the ganglia of the ventral nerve cord. Scale bar indicates 50 μm. B. AG 4 of the 5th instar larva. The peculiarity in localization of one pair of bilateral Mas-AST-IR cell bodies (arrows) and interconnecting axons (arrows) of ventral nerve cord is same as in the AG 1. Magnification is same as in Fig. 9A .

in the 3rd instar larva, in which TG 1 and 2 contained two pairs of Mas-AT-IR cells in the middle and posterior portions, respectively. Thereafter, these Mas-AT-IR cells were detected in the TG during most developmental stages investigated (excluding only prepupal stage). Localization of Mas-AT-IR cell bodies in the TG from the 4th instar larva to 3-day-old pupa was the same as that in the 3rd instar larva. In the 5-day-old pupa and 1-day-old adult in which PTG were formed, however, Mas-AT-IR cells were localized in TG 2 and 3 neuromere and AG 2 neuromere of the PTG. In *D. melanogaster*, Mas-AT-IR cells could be shown in the TG of larva, pupa and adult (Žitňan *et al*., 1993; Yoon and Stay, 1995). In *B. mori,* most of these labeled neurons in the TG showed weak immunoreactivity during all developmental stages and thus axonal projections of these AT-IR neurons could be traced only in part. Therefore, both axonal pathways and function of Mas-AT-IR neurons in each of the three TG remain to be described in detail.

The major new finding in the AG and TAG of *B. mori* was that AG 1 to 7 had Mas-AT-IR fibers in each neuropil, which displayed similarities in the different segments, and there was a projection of axons from these Mas-AT-IR processes into all of the nerves N 1 (or dorsal nerve) and N 2 (or ventral nerve) extending from each of AG 1 to 7. It was assumed that these Mas-AT-IR axons might be derived from one pair of Mas-AT-IR cell bodies in the posteromedian portion of each of AG 1 to 7. In *P. americana* and *Leucophaea maderae*, it has been mentioned that efferent AT-like immunoreactive axons from midline neurons in AG 3-AG6 supply the lateral heart nerves and other neurohemal release sites (Rudwall *et al*., 2000).

ACKNOWLEDGEMENTS

We thank National Institute of Agriculture, Science and Technology (Suwon, Korea) for providing eggs of *Bombyx mori* and Dr. D.R. Nässel (Stockholm University) for the critical readings of this manuscript. We are grateful to Dr. J. A. Veenstra (Universite Bordeaux) and Dr. S. J. Kramer (Sandoz Crop Protection, CA) for providing anti-Mas- AT and anti-Mas-AST antisera. This study was performed by financial supports of both Graduate of Biotechnology, Korea University to Prof. B. H. Lee and Research Institute of Basic Science of Korea University to Dr. M. Y. Kim in 2000.

REFERENCES

Audsley N, Weaver RJ, Edwards JP (1998) Enzyme linked immunosorbent assay for *Manduca sexta* allatostatin (Mas-AS) isolation and measurement of Mas-AS immunoreactive peptide in *Lacanobia oleracea.* Insect Biochem Mol Biol 28: 775–784

Bellés X, Maestro J-L, Piulachs M-D, Johnen AH, Duve H, Thorpe A (1994) Allatostatic neuropeptides from the cockroach *Blattella germanica* (L.) (Dictyoptera, Blattellidae). Identification, immunolocalization and activity. Regul Pept 53: 237–247

Bellés X, Graham LA, Bendena WG, Ding Q, Edwards JP, Weaver RJ, Tobe SS (1999) The molecular evolution of the allatostatin precurosor in cockroaches. Pepties 20: 11–22

Bhatt TR, Horodyski FM (1999) Expression of the *Manduca sexta* allatotropin gene in cells of the central and enteric nervous systems. J Comp Neurol 403: 407–420

Bogus MI, Scheller K (1994) Identification of allatotropin–secreting cells in the brain of an insect larva. Naturwissenschaften 81: 87–89

Bogus M, Scheller K (1996) Allatotropin released by the brain controls larval molting in *Galleria mellonella* by affecting juvenile hormone synthesis. Int J Dev Biol 40: 205–210

Burrows M (1996) The neurobiology of an insect brain. 1st edition, Oxford Univ Press, Oxford

Davis NT, Veenstra JA, Feyereisen R, Hildebrand JG (1997) Allatostatin–like immunoreactive neurons of the tobacco hormworm, *Manduca sexta*, and isolation and identification of a new neuropeptide related to cockroach allatostatins. J Comp Neurol 385: 265–284

Davey M, Duve H, Thorpe A, East P (1999) Characterisation of the helicostatin peptide precursor gene from *Helicoverpa armigera.* Insect Biochem Mol Biol 29: 1119–1127

Ding Q, Donly B.C, Tobe SS, Bendena WG (1995) Comparison of the allatostatin neuropeptide precursors in the distantly related

cockroaches *Periplaneta americana* and *Diploptera punctata*. Eur J Biochem 234: 737–746

Donly BC, Ding Q, Tobe SS, Bendena WG (1993) Molecular cloning of the gene for the allatostatin family of neuropeptides from the cockroach *Diploptera punctata*. Proc Natl Acad Sci USA 90: 8807–8811

Duve H, Johnsen AH, Scott AG, Yu CG, Yagi KJ, Tobe SS, Thorpe A (1993) Callatostatins: neuropeptides from the blowfly *Calliphora vomitoria* with sequence homology to cockroach allatostatins. Proc Natl Acad Sci USA 90: 2456–2460

Duve H, Johnsen AH, Scott AG, East P, Thorpe A (1994) [Hyp^3] Met– callatostatin: Identification and biological properties of a novel neuropeptide from the blowfly *Calliphora vomitoria*. J Biol Chem 269: 21059–21066

Duve H, Thorpe A (1994) Distribution and functional significance of Leu– callatostatins in the blowfly *Calliphora vomitoria*. Cell Tissue Res 276: 367–379

Duve H, Johnsen AH, Maestro J, Scott AG, Crook N, Winstanley D, Thorpe A (1997a) Identification, tissue localization and physiological effect in vitro of a neuroendocrine peptide identical to a dipteran Leu–callatostatin in the codling moth *Cydia pomonella* (Tortricidae : Lepidoptera). Cell Tissue Res 289: 73–83

Duve H, Johnsen AH, Maestro J, Scott AG, Winstanley D, Davey M, East PD, Thorpe A (1997b) Lepidopteran peptides of the allatostain superfamily. Peptides 18: 1301–1309

Hayes TK, Guan X–C, Johnsen V, Strey A, Tobe SS (1994) Structure–activity studies of allatostatin 4 on the inhibition of juvenile hormone biosynthesis by corpora allata. : the importnace of individual side chains and stereochmistry. Peptides 15: 1165–1171

Jin JY, Kwon O, Yu C H, Lee BH (2000) Posttembryonic development of *Diploptera punctata* allatostatin I-immunoreactive neurons in developing brains from the silk moth *Bombyx mori*. Korean J Entomol 30: 43–49

Kataoka H, Toschi A, Li JP, Carney RL, Schooley DA, Kramer SJ (1989) Identification of an allatotropin from adult *Manduca sexta*. Science 243: 1481–1483

Kim MY, Lee BH, Kwon D, Kang H, Nässel DR (1998) Distribution of tachykinin-related neuropeptide in the developing central nervous system of the moth *Spodoptera litura*. Cell Tissue Res 294: 351–365

Kramer SJ, Toschi A, Miller CA, Kataoka H, Quistad GB, Li JP, Carney RL, Schooley DA (1991) Identification of an allatostatin from the tobacco hornworm *Manduca sexta*. Proc Natl Acad Sci USA 88: 9458–9462

Kreissl S, Schulte CC, Agricola HJ, Rathemayer W (1999) A singe allatostatin–immunoreactive neuron innervates skeletal muscles of several segments in the locust. J Comp Neurol 413, 507–519

Lee BH, Kang H, Kwon D, Park CI, Kim WK, Kim MY (1998) Postembryonic development of leucokinin-like immunoreactive neurons in the moth *Spodoptera litura*. Tissue Cell 30: 74–85

Maestro JL, Belles X, Piulachs MD, Thorpe A, Duve H (1998) Localization of allatostatin–immunoreactive material in the central nervous systems, stomatogastric nervous system and gut of the cockroach *Blattella germanica*. Arch Insect Biochem Physiol 37: 269–282

Martin D, Piulachs MD, Belles X (1996) Inhibition of vitellogenin production by allatostatin in the German cockroach. Mol Cell Endocrinol 121: 191–196

Matthias WL, Klaus HH (1995) Allatotropic activity in the suboesophageal ganglia of crickets, *Gryllus bimaculatus* and *Acheta domesticus* (Ensifera: Gryllidae). J Insect Physiol 41: 191–196

Neuhäuser T, Sorge D, Stay B, Hoffman KH (1994). Responsiveness of the adult cricket (*Gryllus bimaculatus* and *Acheta domesticus*) retrocerebral complex to allatostatin-1 from a cockroach, *Dipolptera punctata*. J Comp Physiol B 164: 23–31

Persson MGS, Nässel DR (1999) Neuropeptides in insect sensory neurones: tachykinin-, FMRFamide- and allatotropin-related peptides in terminals of locust thoracic sensory afferents. Brain Res 816: 131–141

Pratt GE, Farnsworth DE, Siegel NR, Fok KF, Feyereisin R (1989) Identification of an allatostatin from adult *Diploptera punctata*. Biochem Biophys Res Comm 16: 1243–1247

Pratt GE, Farnsworth DE, Fok KF, Siegel NR, McCormack AL, Shabanowitz J, Hunt DF, Feyereisen R (1991) Identity of a second type of allatostatin from cockroach brains: an octadecapeptide amide with a tyrosine-rich address sequence. Proc Natl Acad Sci USA 88: 2412–2416

Rankin SM, Stay B, Chan K, Jackson ES (1998) Cockroach allatostatin-immunoreactive neurons and effects of cockroach allatostatin in earwigs. Archs Insect Biochem Physiol 38: 155–165

Rudwall AJ, Sliwowska J, Nässel DR (2000) Allatotropin-like neuropeptide in the cockroach abdominal nervous system: myotropic actions, sexually dimorphic distribution and colocalizaton with serotonin. J Comp Neurol 428: 159–173

Skinner JR, Fairbrain SE, Woodhead AP, Bendena WG, Stay B (1997) Allatostatin in hemocytes of the cockroach *Diploptera punctata*. Cell Tissue Res 290: 119–128

Stay B, Chan KK, Woodhead AP (1992) Allatostatin–immunoreactive neurons projecting to the corpora allata of adult *Diploptera punctata*. Cell Tissue Res 270: 15–23

Stay B, Tobe SS, Bendena WG (1994) Allatostatins : identification, primary structures, functions and distribution. Adv Insect Physiol 25: 267–337

Taylor PA, Bhatt TR, Horodyski FM (1996) Molecular charaterization and expression analysis of *Manduca sexta* allatotropin. Eur J Biochem 239: 588–596

Tobe SS, Stay B (1985) Structure and regulation of the corpora allata. Adv Insect Physiol 18: 305–432

Veelaert D, Schooft L, Tobe SS, Yu CG, Vullings HGB, Couillard F, De Loof A (1995) Immunological evidence for an allatostatin–like neuropeptide in the central neurons system of *Schistocerca gregaria*, *Locusta migratoria* and *Neobellieria bullata*. Cell Tissue Res 279: 601–611

Veelaert D, Devreese B, Schoofs L, Van Beeumen J, Vanden Broeck J, Tobe SS, De Loof A (1996) Isolation and characterization of eight myoinhibiting peptides from the desert locust, *Schistocerca gregaria* : new members of the cockroach allatostatin family. Mol Cell Endocrinol 122: 183–190

Veenstra JA, Hagedorn HH (1993) A sensitive enzyme immuno assay for *Manduca* allatotropin and the existence of an allatotropin-immunoreactive peptide in *Periplaneta americana*. Archs Insect Biochem Physiol 23: 99–109

Veenstra JA, Lehman HK, Davis NT (1994) Allatotropin is a cardioacceleratory peptides in *Manduca sexta*. J Exp Biol 188: 347–354

Veenstra JA, Noriega FG, Graf R, Feyereisen R (1997) Identification of three allatostatins and their cDNA from the mosquito *Aedes aegypti*. Peptides 18: 937–942

Vitzthum H, Homberg U, Agricola H (1996) Distribution of Dip-allatostatin I-like immunoreactivity in the brain of the locust *Schistocerca gregaria* with detaided analysis of immunostainig in the central complex. J Comp Neurol 369: 419–437

Weaver RJ, Freeman ZA, Pickering MG, Edward JP (1994) Identification of two allatostatins from the CNS of the cockroach *Periplaneta americana* novel members of a family of neuropeptide inhibitors of insect juvenile hormone biosynthesis. Comp Biochem Physiol 107C: 119–127

Woodhead AP, Stay B, Seidel SL, Khan MA, Tobe SS (1989) Primary structure of four allatostatins : neuropeptide inhibitors of juvenile hormone synthesis. Proc Natl Acad Sci USA 86: 5997–6001

Woodhead AP, Khan MA, Stay B, Tobe SS (1994) Two new

allatostatins from the brains of *Diploptera punctata*. Insect Biochem Biol 24: 257–263

Yoon JG, Stay B (1995) Immunocytochemical localization of *Diploptera punctata* allatostation-like peptide in *Drosophila melanogaster*. J Comp Neurol 363: 475–488

Žitňan D, Sehnal F, Bryant P (1993) Neurons producing specific neuropeptides in the central nervous system of normal and pupariation-delayed *Drosophila*. Dev Biol 156: 117–135

Žitňan D, Kingan TG, Kramer SJ, Beckage NE (1995) Accumulation of neuropeptides in cerebral neurosecretory system of *Manduca sexta* larvae parasitized by the Braconid Wasp *Cotesia congregata*. J Comp Neurol 356: 83–100

(Received October 16, 2000 / Accepted January 15, 2001)